Biochemistry and Biophysics Reports 17 (2019) 108–113

Contents lists available at ScienceDirect

Biochemistry and Biophysics Reports

journal homepage: www.elsevier.com/locate/bbrep

Hyperinsulinemic hypoglycemia subtype glucokinase V91L mutant induces necrosis in β-cells via ATP depletion

Brian Lu[a,b], Jason M. Tonne[a], Miguel Munoz-Gomez[a], Yasuhiro Ikeda[a,b,*]

[a] Department of Molecular Medicine, Mayo Clinic, Rochester, MN, USA
[b] Virology and Gene Therapy Graduate Program, Mayo Clinic Graduate School of Biomedical Sciences, Rochester, MN 55905, USA

ARTICLE INFO

Keywords:
Glucokinase
Hyperinsulinemic hypoglycemia subtype glucokinase
Beta-cell death
Hyperinsulinemic hypoglycemia
Necrosis

ABSTRACT

Hyperinsulinemic hypoglycemia subtype glucokinase (GCK-HH) is caused by an activating mutation in glucokinase (GCK) and has been shown to increase β-cell death. However, the mechanism of β-cell death in GCK-HH remains poorly understood. Here, we expressed the GCK-HH V91L GCK mutant in INS-1 832/13 cells to determine the effect of the mutation on β-cell viability and the mechanisms of β-cell death. We showed that expression of the V91L GCK mutant in INS-1 832/13 cells resulted in a rapid glucose concentration-dependent loss of cell viability. At 11 mM D-glucose, INS-1 832/13 cells expressing V91L GCK showed increased cell permeability without significant increases in Annexin V staining or caspase 3/7 activation, indicating that these cells are primarily undergoing cell death via necrosis. Over-expression of SV40 large T antigen, which inhibits the p53 pathway, did not affect the V91L GCK-induced cell death. We also found that non-phosphorylatable L-glucose did not induce rapid cell death. Of note, glucose phosphorylation coincided with a 90% loss of intracellular ATP content. Thus, our data suggest that the GCK V91L mutant induces rapid necrosis in INS-1 cells through accelerated glucose phosphorylation, ATP depletion, and increased cell permeability.

1. Introduction

By catalyzing the rate-limiting glucose phosphorylation step in β-cell glucose metabolism, glucokinase (GCK), functions as the glucose sensor within β-cells for regulating glucose-stimulated insulin secretion (GSIS). GCK, through its central role in glucose metabolism, also indirectly regulates β-cell proliferation [1,2]. As such, mutations resulting in changes in GCK activity can have profound effects on β-cell function. Mutations resulting in GCK deficiency causes of maturity onset diabetes of the young (GCK-MODY) while activating GCK mutations cause hyperinsulinemic hypoglycemia (GCK-HH) [3]. Patients with GCK-MODY generally do not require treatment [3–5]. However treatment for patients with GCK-HH depends on the severity of hypoglycemia and can range from diazoxide to partial pancreatectomy [6,7].

The GCK mutations in GCH-HH activates GCK by increasing GCK's affinity for glucose [6–12]. This enhances β-cell glycolytic flux and increases GSIS. However, excessive glycolytic flux has also been shown to increase β-cell toxicity [13,14]. Indeed, pancreas samples from a patient with the V91L GCK-HH mutation also showed increased TUNEL staining in β-cells. However, while Tornovsky-Babeay et al. demonstrated that the Y214C GCK-HH mutation induces apoptosis in β-cells via p53 activation [14], it remains unclear if other GCK-HH mutations would share the same mechanisms of β-cell toxicity.

In this study, we expressed the GCK-HH GCK V91L activating mutant in rat β-cells in vitro. Our results demonstrate that β-cells expressing V91L GCK are acutely sensitive to glucose, leading to rapid cell death via depletion of intracellular ATP and necrosis.

2. Materials and methods

2.1. Cells

HEK293T cells were purchased from ATCC (Manassas, VA, USA) and cultured in DMEM supplemented with 10% FBS, 50 U/ml penicillin, and 50 μg/ml streptomycin. INS-1 832/13 cells were a generous gift from Dr. Aleksey Matveyenko. INS-1 832/13 cells and INS-1 832/13 cells expressing GCK were cultured in RPMI supplemented with 10% FBS, 10 mM HEPES, 1 mM sodium pyruvate, 50 μM beta-mercaptoethanol, 50 U/ml penicillin, and 50 μg/ml streptomycin. INS-1832/13 cells expressing V91L GCK were cultured in glucose-free RPMI supplemented with 10% FBS, 10 mM HEPES, 1 mM sodium pyruvate, 50 μM beta-mercaptoethanol, 50 U/ml penicillin, and 50 μg/ml streptomycin.

* Correspondence to: Department of Molecular Medicine, Mayo Clinic College of Medicine, 200 First Street SW, Rochester, MN 55905, USA.
E-mail address: ikeda.yasuhiro@mayo.edu (Y. Ikeda).

https://doi.org/10.1016/j.bbrep.2018.12.002
Received 15 August 2018; Received in revised form 9 November 2018; Accepted 6 December 2018
Available online 20 December 2018

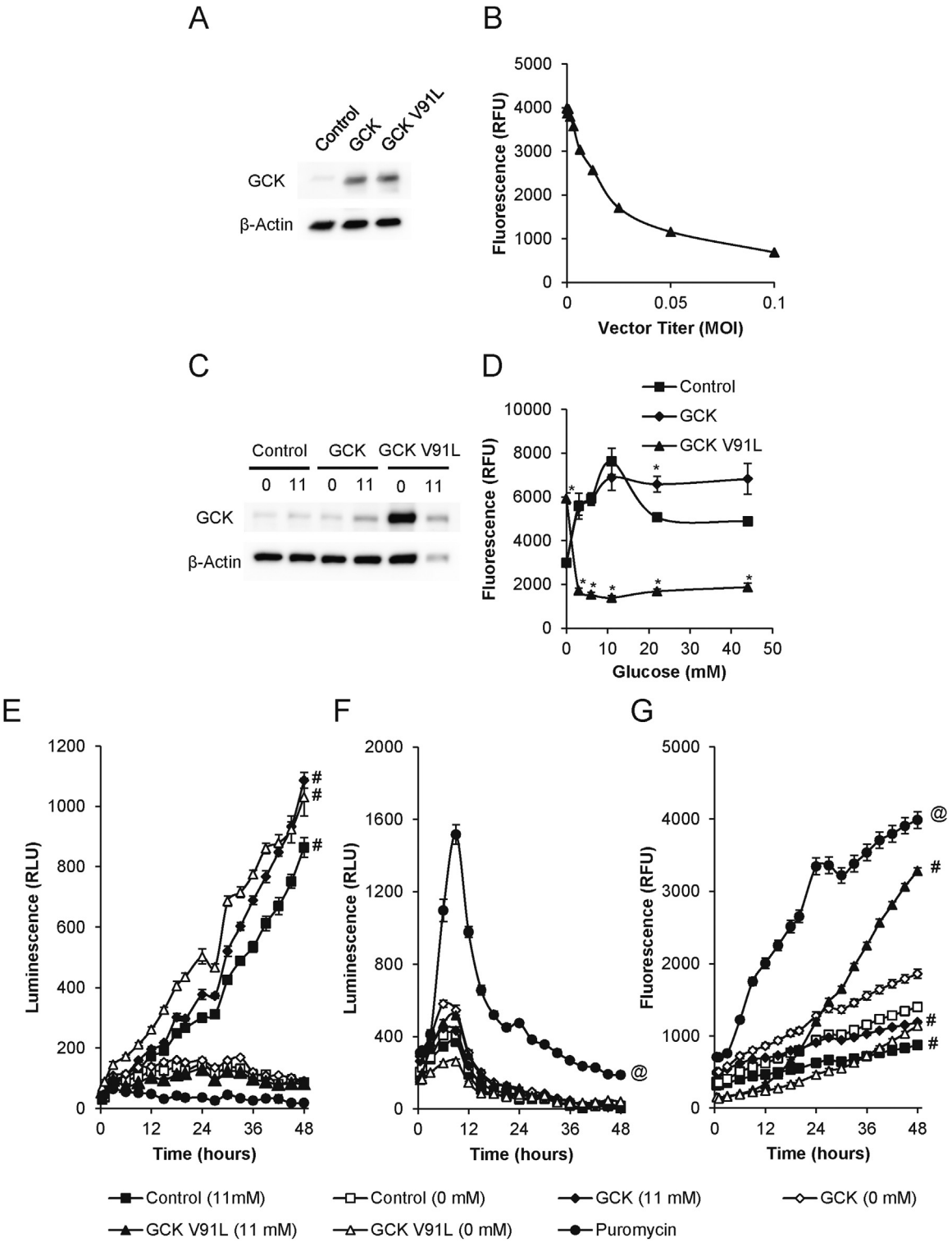

Fig. 1. V91L GCK expression in INS-1 832/13 cells induces D-glucose-dependent cell death. (A) Immunoblot of HEK293T cells transduced with SIN-SFFV-GCK or SIN-SFFV-GCK-V91L and selected by puromycin. (B) Cell viability of INS-1 832/13 cells transduced with increasing SIN-SFFV-GCK-V91L vector titers and cultured with 11 mM D-glucose for 48 h after transduction (n = 8 per vector titer). (C) Immunoblot of non-transduced INS-1 832/13 cells and INS-1 832/13 cells transduced with SIN-SFFV-GCK or SIN-SFFV-GCK-V91L following puromycin selection. (D) Cell viability of non-transduced control INS-1 832/13 cells, INS-1 832/13 GCK cells, and INS-1 832/13 GCK V91L cells after culturing in increasing D-glucose concentrations for 24 h (n = 4 per group). (E) Real-time cell viability of INS-1 832/13, INS-1 832/13 GCK, and INS-1 832/13 GCK V91L cultured with 0 mM and 11 mM D-glucose (n = 6–7 per group). (F) Real-time Annexin V luminescence of INS-1 832/13, INS-1 832/13 GCK, and INS-1 832/13 GCK V91L cultured with 0 mM and 11 mM D-glucose (n = 6–7 per group). (G) Real-time cell permeability of INS-1 832/13, INS-1 832/13 GCK, and INS-1 832/13 GCK V91L cultured with 0 mM and 11 mM D-glucose (n = 6–7 per group). Real-time cell viability, Annexin V luminescence, and cell permeability measurements were taken 30 min, 1 h, and every 3 h after glucose addition for 48 h. Puromycin was supplemented at 25 μg/ml media as a positive cell death control. Results shown as line graphs with mean ± SEM. *$p < 0.05$ against control, # $p < 0.05$ against respective 0 mM D-glucose group, @ $p < 0.05$ against all other groups.

2.2. Plasmids

Wild-type GCK-expressing lentiviral vector was generated as previously described [28]. Briefly, the mouse GCK encoding sequence (GenBank# BC011139.1) was amplified by PCR and cloned into the BamHI-NotI site of pHRSINCSGW_PGRPuro [29], resulting in pSIN-SFFV-GCK. To generate the V91L GCK-expressing lentiviral vector, the V91L mutation was introduced into the pSIN-SFFV-GCK plasmid by site-directed mutagenesis, resulting in pSIN-SFFV-GCK-V91L. Introduction of the V91L mutation was verified by Sanger sequencing. Lentiviral vector expressing the SV40 small and large T antigens, pLenti CMV/TO SV40 small + Large T, was a generous gift from Dr. Eric Campeau through Addgene (#22298, unpublished; Cambridge, MA, USA)

2.3. Lentiviral vector production

Lentiviral vectors were produced by 3 plasmid transfection as previously described with minor modifications [30]. Briefly, the vector plasmid pSIN-SFFV-GCK or pSIN-SFFV-GCK-V91L was co-transfected into HEK293T cells with packaging plasmids Ex-QV and pMD-G. Lentiviral vectors were purified by filtration and concentrated by ultracentrifugation. Lentiviral vectors were titered on HEK293T cells using the colony formation titering method with puromycin. Vector transgene expression was confirmed by immunoblot as previously described with minor modifications [31].

2.4. In vitro studies with INS-1 832/13 cells

Wild-type GCK expressing INS-1 832/13 cells and V91L GCK expressing INS-1 832/13 cells were generated by transducing INS-1 832/13 cells with lentiviral vectors expressing mouse GCK (SIN-SFFV-GCK) or mouse V91L GCK (SIN-SFFV-GCK-V91L), followed by puromycin selection. Vector transgene expression was confirmed via immunoblot as previously described with minor modifications [31]. Immunoblots were imaged using the biostep CELVIN S Chemiluminescence Imager with the biostep SnapAndGo software (ver. 162 rev. 10; Burkhardtsdorf, Germany). Cell viability was measured using the PrestoBlue Cell Viability Reagent (Thermo Fisher Scientific, Waltham, MA, USA) and the RealTime-Glo MT Cell Viability Assay (Promega, Madison, WI, USA) at the indicated times. Annexin V and cell permeability was measured using the RealTime-Glo Annexin V Apoptosis and Necrosis Assay (Promega, Madison, WI, USA) at the indicated times. Puromycin at 25 μg/ml was used as a positive cell death control for the RealTime-Glo MT Cell Viability Assay (Promega, Madison, WI, USA) and the RealTime-Glo Annexin V Apoptosis and Necrosis Assay (Promega, Madison, WI, USA). Cellular ATP was measured using the Luminescent ATP Detection Assay Kit (Abcam) 1 h after glucose addition.

2.5. Live-cell fluorescent microscopy

Live-cell imaging of INS-1 832/13 cells and INS-1 832/13 GCK V91L cells was performed using the Nikon Biostation IM-Q (Nikon, Tokyo, Japan). 3×10^5 INS-1 832/13 cells or INS-1 832/13 GCK V91L cells were seeded in each chamber of ibidi imaging μ-Dish Quad dishes (ibidi, Martinsried, Germany) with 300 μl media and allowed to adhere overnight. The following morning, the media in each chamber were changed to 0 mM D-glucose media or 11 mM D-glucose media. Caspase-3/7 activation was visualized using the CellEvent Caspase-3/7 Green

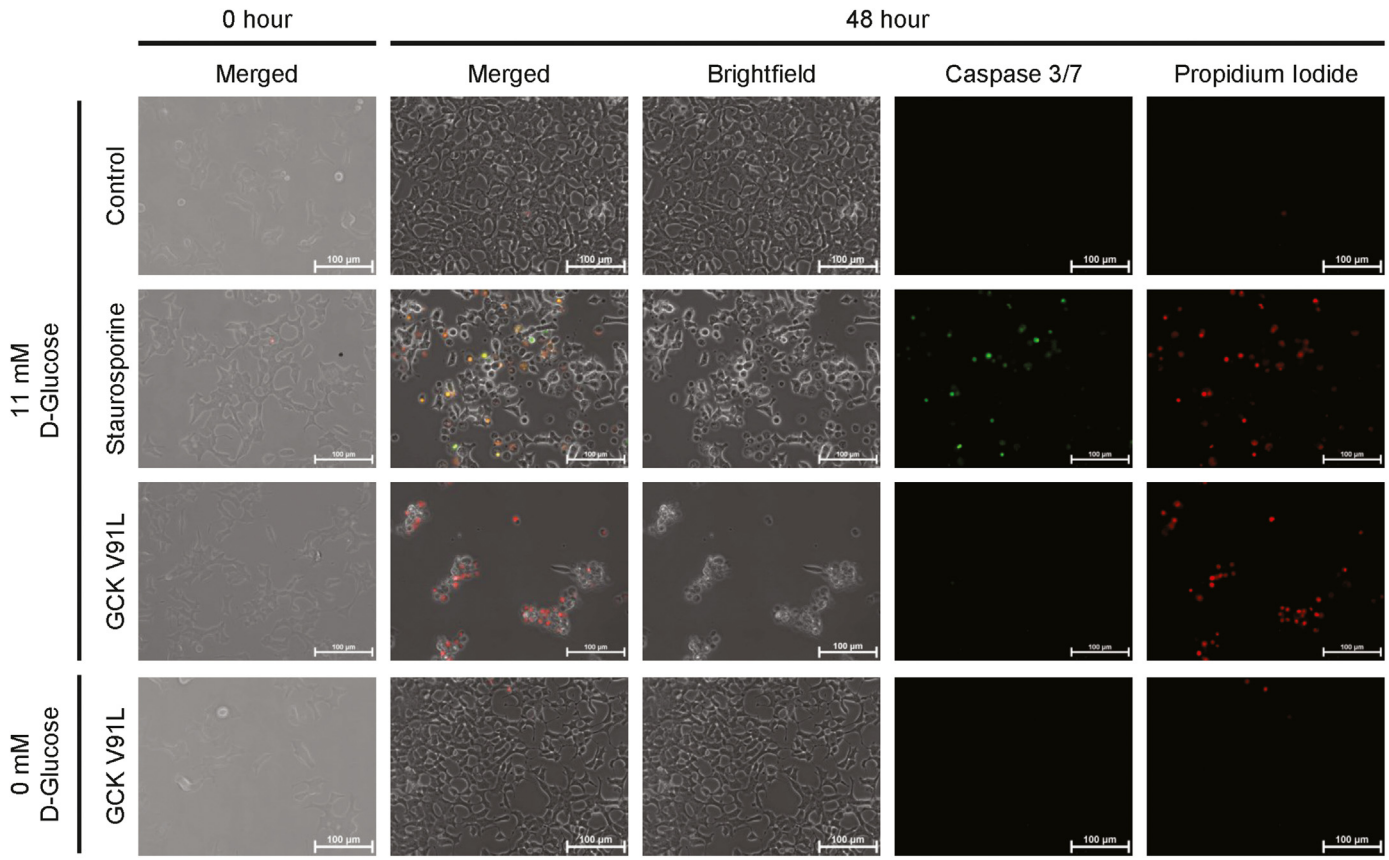

Fig. 2. D-glucose-induces cell death in INS-1 832/13 GCK V91L cells with minimal caspase 3/7 activation. Representative images from fluorescent live-cell imaging taken at 0 h and 48 h after media change. Non-transduced INS-1 832/13 control cells and INS-1 832/13 GCK V91L cells were imaged with 0 mM or 11 mM D-glucose. Caspase 3/7 activation was visualized using CellEvent Caspase-3/7 Green Detection Reagent (Invitrogen). Propidium iodide staining was visualized using the pSIVA Real-Time Apoptosis Fluorescent Microscopy Kit (Bio-Rad). Scale bar represents 100 μm.

Detection Reagent (Invitrogen, Carlsbad, CA, USA). Propidium iodide staining was visualized using the pSIVA Real-Time Apoptosis Fluorescent Microscopy Kit (Bio-Rad Laboratories, Hercules, CA, USA). Images were acquired using the BioStation IM (ver. 2.21 build 144, Nikon, Tokyo, Japan) and processed using the NIS Elements BR software (ver. 3.22.14 build 736, Nikon, Tokyo, Japan).

2.6. Data analysis

Data presented as line graphs or bar graphs with mean ± standard measure of means (SEM). Data were analyzed using the JMP software (ver. 13.0.0; SAS Institute, Cary NC, USA). Statistical significance was determined using the 2-tailed student's *t*-test or repeated measure analysis of variance (ANOVA). Multiple comparisons were analyzed by one way ANOVA followed by two-tailed student's *t*-test with Bonferroni correction. Significance was determined at $p < 0.05$.

3. Results

3.1. V91L GCK expression induces D-glucose-dependent cell death in INS-1 832/13 cells

To express V91L GCK in INS-1 832/13 cells, we constructed lentiviral vectors expressing wild-type GCK and V91L GCK, SIN-SFFV-GCK and SIN-SFFV-GCK-V91L, respectively. To verify expression of transgene upon transduction, we transduced HEK293T cells with SIN-SFFV-GCK or SIN-SFFV-GCK-V91L followed by selection by puromycin. Expression of GCK and V91L GCK after vector transduction was confirmed via immunoblot of transduced HEK293T cells (Fig. 1A). Transduction of INS-1 832/13 cells with increasing vector titers of SIN-SFFV-GCK-V91L showed that cell viability decreases with increasing vector titer (Fig. 1B). We then established INS-1 832/13 cell lines expressing GCK or V91L GCK by transduction with SIN-SFFV-GCK and SIN-SFFV-GCK-V91L, respectively, followed by puromycin selection. Transgene expression in the resulting INS-1 832/13 GCK and INS-1 832/13 GCK V91L cells were verified by immunoblot (Fig. 1C). INS-1 832/13 GCK V91L cells showed decreased cell viability compared to non-transduced controls in all D-glucose concentrations tested except 0 mM D-glucose (Fig. 1D). In comparison, INS- 832/13 GCK cells had increased cell

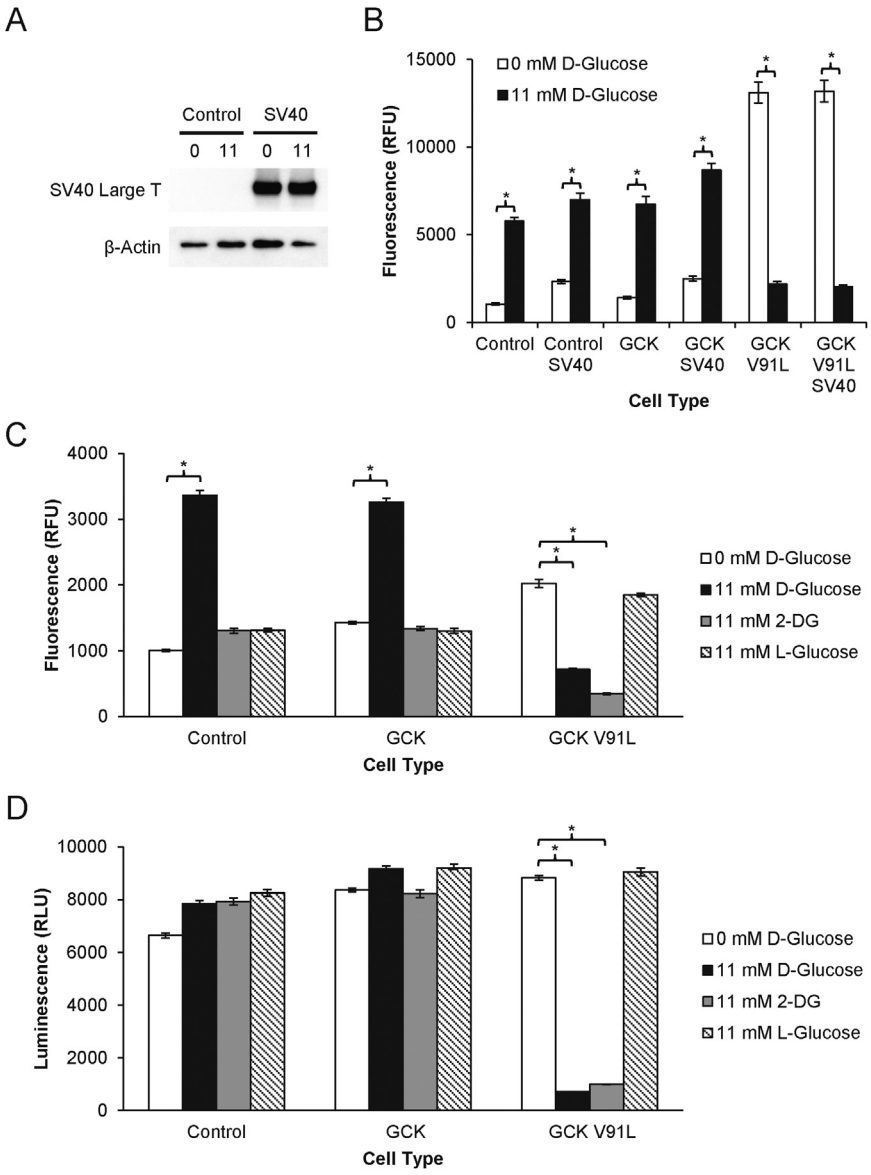

Fig. 3. Glucose phosphorylation is required for D-glucose-induced cell death in INS-1 832/13 GCK V91L cells. (A) Immunoblot of INS-1 832/13 cells transduced with lentiviral vectors expressing the SV40 small and large T antigens. (B) Cell viability of non-transduced INS-1 832/13 cells, INS-1 832/13 GCK cells, and INS-1 832/13 GCK V91L cells 48 h after transduction with lentiviral vectors expressing the SV40 small and large T antigens in 0 mM or 11 mM D-glucose (n = 7 per group). (C) Cell viability of non-transduced INS-1 832/13 cells, INS-1 832/13 GCK cells, and INS-1 832/13 GCK V91L cells cultured for 24 h with 0 mM D-glucose, 11 mM D-glucose, 11 mM 2-DG, or 11 mM L-glucose (n = 7 per group). (D) Intracellular ATP content of non-transduced INS-1 832/13 cells, INS-1 832/13 GCK cells, and INS-1 832/13 GCK V91L cells after 1 h culture with 0 mM D-glucose, 11 mM D-glucose, 11 mM 2-DG, or 11 mM L-glucose (n = 7 per group). Results shown as bar graph with mean ± SEM. *p < 0.05.

viability when cultured at 22 mM D-glucose (Fig. 1D). To determine the mechanism of D-glucose-induced toxicity on INS-1 832/13 cells expressing V91L GCK, cell viability, Annexin V luminescence, and cell permeability in non-transduced INS-1 832/13 control cells, INS-1 832/13 GCK cells, and INS-1832/13 GCK V91L cells were measured in real-time. All cells showed similar differences in growth kinetics when cultured in 0 mM D-glucose compared to 11 mM D-glucose (Fig. 1E). However, while INS-1 832/13 non-transduced cells and INS-1 832/13 GCK cells had positive growths with 11 mM D-glucose and negligible growth with 0 mM D-glucose, INS-1 832/13 GCK V91L cells showed the opposite trend with positive growth with 0 mM D-glucose and negligible growth with 11 mM D-glucose (Fig. 1E). Analysis of Annexin V luminescence intensity in real-time showed slightly elevated luminescence approximately 9 h after D-glucose addition in all cells. However, the luminescence from all cells lines were still significantly lower than that of the 25 μg/ml puromycin positive control. Similarly, cell permeability of the 25 μg/ml puromycin positive control was significantly higher than all other cell lines. But notably, cell permeability of INS-1 832/13 GCK V91L cells in 11 mM D-glucose increased rapidly 24 h after media change, suggesting an increase in necrosis. These results suggest that the decrease in cell viability observed in INS-1 832/13 GCK V91L cells with 11 mM D-glucose is primarily due to increased cell death via necrosis.

3.2. D-glucose induces primarily necrosis in INS-1 832/13 cells expressing V91L GCK

To verify that D-glucose induces primarily necrosis rather than apoptosis in INS-1 832/13 GCK V91L cells, cells were imaged every hour for 48 h after addition of D-glucose. Both non-transduced INS-1 832/13 cells cultured in 11 mM D-glucose and INS-1 832/13 GCK V91L cells cultured in 0 mM D-glucose showed minimal 3/7 activation and negligible changes in cell permeability (Fig. 2, Supplemental Video 1, 4). Non-transduced INS-1 832/13 cells cultured with 11 mM D-glucose and 100 nM staurosporine showed widespread caspase 3/7 activation and increased cell permeability (Fig. 2, Supplemental Video 2). INS-1 832/13 GCK V91L cells cultured in 11 mM D-glucose showed increase cell permeability and minimal caspase 3/7 activation (Fig. 2, Supplemental Video 3). These results further indicate that D-glucose induces cell death primarily via necrosis in INS-1 832/13 GCK V91L cells.

Supplementary material related to this article can be found online at doi:10.1016/j.bbrep.2018.12.002.

3.3. Phosphorylation of D-glucose is required for D-glucose-induced cell death in INS-1 832/13 cells expressing V91L GCK

To determine if p53 activation is involved in D-glucose-induced cell death in INS-1 832/13 GCK V91L cells, we expressed the simian virus 40 (SV40) small and large T antigens via lentiviral transduction. Expression of the SV40 large T antigen in INS-1 832/13 cells following transduction with lentiviral vectors was confirmed via immunoblot (Fig. 3A). Transduction with lentiviral vectors expressing the SV40 small and large T antigens did not rescue INS-1 832/13 GCK V91L cells from D-glucose-induced cell death (Fig. 3B), suggesting that p53 activation is not the primary mechanism of cell death. To determine if glucose metabolism was required for induction of necrosis, we cultured non-transduced control INS-1 832/13 cells, INS-1 832/13 GCK cells, and INS-1 832/13 GCK V91L cells with 0 mM D-glucose, 11 mM D-glucose, 11 mM 2-deoxyglucose (2-DG), or 11 mM L-glucose. Culture of INS-1 832/13 GCK V91L cells in 11 mM 2-DG, which can be phosphorylated but not further metabolized, led to a similar decrease in cell viability as culture in 11 mM D-glucose (Fig. 3C). Culture of INS-1 832/13 GCK V91L cells in 11 mM of the non-phosphorylatable L-glucose, however, did not result in loss of cell viability (Fig. 3C). This indicates that glucose phosphorylation, but not glucose metabolism, is required for glucose-induced cell death in INS-1 832/13 GCK V91L cells. As glucose phosphorylation consumes ATP, we measured the intracellular ATP contents of INS-1 832/13 cells, INS-1 832/13 GCK cells, and INS-1 832/13 GCK V91L cells cultured with 0 mM D-glucose, 11 mM D-glucose, 11 mM 2-deoxyglucose (2-DG), or 11 mM L-glucose. Culture of INS-1 832/13 GCK V91L cells with 11 mM D-glucose or 2-DG resulted in the loss of over 90% of ATP content within 1 h while culture with 11 mM L-glucose did not lead to changes in cellular ATP content (Fig. 3D). These results suggest that the hyperactive V91L GCK induces cell death by depleting cellular ATP and increasing cell permeability.

4. Discussion

To date, 15 GCK-HH mutations have been identified [3,7,15,16]. However, only the V91L GCK mutation has been associated with β-cell death in humans [7]. Pancreas sections from the patient with the V91L GCK mutation showed enlarged islets, enhanced β-cell proliferation, and increased β-cell TUNEL staining [7]. The enlarged islets is likely the result of the enhanced β-cell proliferation from increased glycolytic flux [7], as glucose has been shown to be a potent regulator of β-cell proliferation [1,2,17]. The mechanism of β-cell death in β-cells carrying the V91L GCK mutation remains unknown. Our results in vitro propose a mechanism of cell death via necrosis in these cells.

Our results showed that β-cell expressing V91L GCK undergo glucose phosphorylation-dependent necrosis coincident with ATP depletion, suggesting that, in the presence of excess D-glucose, the hyperactive V91L GCK consumed intracellular ATP for glucose phosphorylation faster than ATP can be replenished via downstream glucose metabolism. This excess glucose phosphorylation likely results in accumulation of glucose 6-phosphate, and its conversion product fructose 6-phosphate, similar to what was observed by Wang and Iynedjian in INS-r3GK27 cells expressing wild-type GCK 20-fold above normal [13]. However, our results showed a more complete depletion of intracellular ATP (90% vs. 75%) and a more rapid morphological change (< 1 h vs. 16 h) compared to what was observed by Wang and Iynedjian [13], likely due to the higher enzymatic kinetics of the V91L GCK mutant [7]. It is possible the accumulation of glucose 6-phosphate and fructose 6-phosphate may result in osmotic stress-induced necrosis due to the osmotic intake of water. However, previous studies from another cell line suggest against this possibility. Similar, rapid morphological changes upon ATP depletion have been observed the ROC-1 glial cell line by Jurkowitz-Alexander et al. [18]. Inhibition of the Na^+, K^+-ATPase pump in ROC-1 cells results in accumulation of Na^+ and Cl^- ions and promotes osmotic swelling [18]. However, osmotic swelling following inhibition of the Na^+, K^+-ATPase pump, though inducing similar morphological changes as ATP depletion, did not result in necrosis [18]. The level of ATP depletion we observed in β-cell expressing V91L GCK is also consistent with previously reported level of ATP depletion required for induction of necrosis. ATP depletion, therefore, is likely the primary cause of necrosis in β-cell expressing V91L GCK.

While TUNEL staining is traditionally thought to be an apoptosis marker, studies have shown that TUNEL can stain necrotic cells [19–21]. Furthermore, DNA degradation has also been observed in necrotic cells [22]. TUNEL staining alone is therefore insufficient to distinguish apoptosis from necrosis. To distinguish apoptosis from necrosis in our in vitro model, we conducted kinetic analyses of Annexin V staining, cell permeability, and caspase 3/7 activation. Based on these combined parameters, our results indicate that β-cells expressing V91L GCK primarily undergo cell death via necrosis.

Clinical presentations of the patient with V91L GCK mutation were similar to those of the patient with Y214C GCK mutation. Both patients showed increased β-cell area and severe hypoglycemia requiring partial pancreatectomy [6,7] While β-cell death was not assessed in the patient with Y214C GCK mutation [6], transgenic mice carrying the Y214C GCK mutation had increased β-cell apoptosis from DNA damage and subsequent p53 activation [14]. Our results in vitro using the SV40 large T antigen suggests a mechanism of cell death independent of p53

with the V91L GCK mutant. This implies that the mechanism of cell death observed with the V91L GCK mutation may be different from those observed with the Y214C GCK mutation. The difference in cell death mechanism may be due to the severity of ATP depletion. Intracellular ATP is required for apoptosis [23,24], and ATP depletion greater than 85% has been shown to divert the cell death pathway from apoptosis to necrosis [25–27]. As such, necrosis induced by the V91L GCK mutant is likely not specifically due to the V91L mutation, but rather the resulting high level of GCK activity. It should be noted, however, that further studies with the V91L GCK mutant are required to verify our findings. Particularly, our results remain to be validated in an in vivo model.

In summary, our data show a novel mechanism of β-cell death in GCK-HH. The V91L mutation in GCK-HH results in β-cell death via necrosis following ATP depletion in a glucose phosphorylation-dependent manner.

Disclosures

No potential conflicts of interest relevant to this article were reported.

CRediT authorship contribution statement

Brian Lu: Conceptualization, Data curation, Formal analysis, Investigation, Methodology, Software, Validation, Visualization, Writing - original draft, Writing - review & editing. **Jason M. Tonne:** Data curation, Investigation, Resources, Writing - review & editing. **Miguel Munoz-Gomez:** Data curation, Investigation, Resources, Writing - review & editing. **Yasuhiro Ikeda:** Funding acquisition, Project administration, Resources, Supervision, Writing - review & editing.

Acknowledgements

The authors would like to thank the Mayo Clinic Graduate School of Biomedical Sciences and the Initiative for Maximizing Student Development for supporting our Ph.D. trainees.

Funding

This work was supported by the Vann Family Fund in Diabetes Research, Kieckhefers Foundation, Paul A. and Ruth M. Schilling Medical Research Endowment Fund, and Mayo Clinic Center for Regenerative Medicine (to YI), and Mayo Clinic Graduate School of Biomedical Sciences (to BL), and Initiative for Maximizing Student Development (IMSD, to BL).

Appendix A. Transparency document

Supplementary data associated with this article can be found in the online version at doi:10.1016/j.bbrep.2018.12.002.

References

[1] S.J. Salpeter, A. Klochendler, N. Weinberg-Corem, S. Porat, et al., Glucose regulates cyclin D2 expression in quiescent and replicating pancreatic β-cells through glycolysis and calcium channels, Endocrinology 152 (2011) 2589–2598, https://doi.org/10.1210/en.2010-1372.

[2] S. Porat, N. Weinberg-Corem, S. Tornovsky-Babaey, R. Schyr-Ben-Haroush, et al., Control of pancreatic β cell regeneration by glucose metabolism, Cell Metab. 13 (2011) 440–449, https://doi.org/10.1016/j.cmet.2011.02.012.

[3] K.K. Osbak, K. Colclough, C. Saint-Martin, N.L. Beer, et al., Update on mutations in glucokinase (*GCK*), which cause maturity-onset diabetes of the young, permanent neonatal diabetes, and hyperinsulinemic hypoglycemia, Hum. Mutat. 30 (2009) 1512–1526, https://doi.org/10.1002/humu.21110.

[4] A. Stride, B. Shields, O. Gill-Carey, A.J. Chakera, et al., Cross-sectional and longitudinal studies suggest pharmacological treatment used in patients with glucokinase mutations does not alter glycaemia, Diabetologia 57 (2014) 54–56, https://doi.org/10.1007/s00125-013-3075-x.

[5] A.J. Chakera, A.M. Steele, A.L. Gloyn, M.H. Shepherd, et al., Recognition and management of individuals with hyperglycemia because of a heterozygous glucokinase mutation, Diabetes Care 38 (2015) 1383–1392, https://doi.org/10.2337/dc14-2769.

[6] A.L. Cuesta-Muñoz, H. Huopio, T. Otonkoski, J.M. Gomez-Zumaquero, et al., Severe persistent hyperinsulinemic hypoglycemia due to a de novo glucokinase mutation, Diabetes 53 (2004) 2164–2168, https://doi.org/10.2337/diabetes.53.8.2164.

[7] S. Kassem, S. Bhandari, P. Rodríguez-Bada, R. Motaghedi, et al., Large islets, beta-cell proliferation, and a glucokinase mutation, New Engl. J. Med. 362 (2010) 1348–1350, https://doi.org/10.1056/NEJMc0909845.

[8] B. Glaser, P. Kesavan, M. Heyman, E. Davis, et al., Familial hyperinsulinism caused by an activating glucokinase mutation, New Engl. J. Med. 338 (1998) 226–260, https://doi.org/10.1056/NEJM199801223380404.

[9] S. Sayed, D.R. Langdon, S. Odili, P. Chen, et al., Extremes of clinical and enzymatic phenotypes in children with hyperinsulinism caused by glucokinase activating mutations, Diabetes 58 (2009) 1419–1427, https://doi.org/10.2337/db08-1792.

[10] M. Wabitsch, G. Lahr, M. Van de Bunt, C. Marchant, et al., Heterogeneity in disease severity in a family with a novel G68V GCK activating mutation causing persistent hyperinsulinaemic hypoglycaemia of infancy, Diabet. Med. 24 (2007) 1393–1399, https://doi.org/10.1111/j.1464-5491.2007.02285.x.

[11] H.B.T. Christesen, N.D. Tribble, A. Molven, J. Siddiqui, et al., Activating glucokinase (GCK) mutations as a cause of medically responsive congenital hyperinsulinism: prevalence in children and characterisation of a novel GCK mutation, Eur. J. Endocrinol. 159 (2008) 27–34, https://doi.org/10.1530/EJE-08-0203.

[12] A.L. Gloyn, K. Noordam, M.A.A.P. Willemsen, S. Ellard, et al., Insights into the biochemical and genetic basis of glucokinase activation from naturally occurring hypoglycemia mutations, Diabetes 52 (2003) 2433–2440, https://doi.org/10.2337/diabetes.52.9.2433.

[13] H. Wang, P.B. Iynedjian, Acute glucose intolerance in insulinoma cells with unbalanced overexpression of glucokinase, J. Biol. Chem. 272 (1997) 25731–25736, https://doi.org/10.1074/jbc.272.41.25731.

[14] S. Tornovsky-Babeay, D. Dadon, O. Ziv, E. Tzipilevich, et al., Type 2 diabetes and congenital hyperinsulinism cause dna double-strand breaks and p53 activity in β cells, Cell Metab. 19 (2014) 109–121, https://doi.org/10.1016/j.cmet.2013.11.007.

[15] N.L. Beer, M. van de Bunt, K. Colclough, C. Lukacs, et al., Discovery of a novel site regulating glucokinase activity following characterization of a new mutation causing hyperinsulinemic hypoglycemia in humans, J. Biol. Chem. 286 (2011) 19118–19126, https://doi.org/10.1074/jbc.M111.223362.

[16] F. Barbetti, N. Cobo-Vuilleumier, C. Dionisi-Vici, S. Toni, et al., Opposite clinical phenotypes of glucokinase disease: description of a novel activating mutation and contiguous inactivating mutations in human glucokinase (GCK) gene, Mol. Endocrinol. 23 (2009) 1983–1989, https://doi.org/10.1210/me.2009-0094.

[17] R.E. Stamateris, R.B. Sharma, Y. Kong, P. Ebrahimpour, et al., Glucose induces mouse β-cell proliferation via IRS2, MTOR, and cyclin D2 but not the insulin receptor, Diabetes 65 (2016) 981–995, https://doi.org/10.2337/db15-0529.

[18] M.S. Jurkowitz-Alexander, R.A. Altschuld, C.M. Hohl, J.D. Johnson, et al., Cell swelling, blebbing, and death are dependent on ATP depletion and independent of calcium during chemical hypoxia in a glial cell line (ROC-1), J. Neurochem. 59 (1992) 344–352, https://doi.org/10.1111/j.1471-4159.1992.tb08910.x.

[19] B.G. Kraupp, B. Ruttkay-Nedecky, H. Koudelka, K. Bukowska, et al., In situ detection of fragmented DNA (TUNEL assay) fails to discriminate among apoptosis, necrosis, and autolytic cell death: a cautionary note, Hepatology 21 (1995) 1465–1468, https://doi.org/10.1002/hep.1840210534.

[20] C. de Torresa, F. Munella, I. Ferrerc, J. Reventósa, A. Macayaab, Identification of necrotic cell death by the TUNEL assay in the hypoxic-ischemic neonatal rat brain, Neurosci. Lett. 230 (1997) 1–4, https://doi.org/10.1016/S0304-3940(97)00445-X.

[21] C. Artus, H. Boujrad, A. Bouharrour, M.N. Brunelle, et al., AIF promotes chromatinolysis and caspase-independent programmed necrosis by interacting with histone H2AX, EMBO J. 29 (2010) 1585–1599, https://doi.org/10.1038/emboj.2010.43.

[22] V.V. Didenko, H. Ngo, D.S. Baskin, Early necrotic DNA degradation: presence of blunt-ended DNA breaks, 3′ and 5′ overhangs in apoptosis, but only 5′ overhangs in early necrosis, Am. J. Pathol. 162 (2003) 1571–1578, https://doi.org/10.1016/S0002-9440(10)64291-5.

[23] M.V. Zamaraeva, R.Z. Sabirov, E. Maeno, Y. Ando-Akatsuka, et al., Cells die with increased cytosolic ATP during apoptosis: a bioluminescence study with intracellular luciferase, Cell Death Differ. 12 (2005) 1390–1397, https://doi.org/10.1038/sj.cdd.4401661.

[24] T. Tatsumi, J. Shiraishi, N. Keira, K. Akashi, et al., Intracellular ATP is required for mitochondrial apoptotic pathways in isolated hypoxic rat cardiac myocytes, Cardiovasc. Res. 59 (2003) 428–440, https://doi.org/10.1016/S0008-6363(03)00391-2.

[25] N. Miyoshi, E. Watanabe, T. Osawa, M. Okuhira, et al., ATP depletion alters the mode of cell death induced by benzyl isothiocyanate, Biochem. Biophys. Acta 2008 (1782) 566–573, https://doi.org/10.1016/j.bbadis.2008.07.002.

[26] Y. Eguchi, S. Shimizu, Y. Tsujimoto, Intracellular ATP levels determine cell death fate by apoptosis or necrosis, Cancer Res. 57 (1997) 1835–1840.

[27] W. Lieberthal, S.A. Menza, J.S. Levine, Graded, ATP depletion can cause necrosis or apoptosis of cultured mouse proximal tubular cells, Am. J. Physiol. 274 (1998) F315–F327.

[28] B. Lu, M. Munoz-Gomez, Y. Ikeda, The two major glucokinase isoforms show conserved functionality in β-cells despite different subcellular distribution, Biol. Chem. 399 (2018) 565–576, https://doi.org/10.1515/hsz-2018-0109.

[29] T. Sakuma, J.I. Davila, J.A. Malcolm, J.-P.A. Kocher, et al., Murine Leukemia Virus uses NXF1 for nuclear export of spliced and unspliced viral transcripts, J. Virol. 88 (2014) 4069–4082, https://doi.org/10.1128/JVI.03584-13.

[30] J.M. Tonne, J.M. Campbell, A. Cataliotti, S. Ohmine, et al., Secretion of glycosylated Pro–B-type natriuretic peptide from normal cardiomyocytes, Clin. Chem. 57 (2011) 864–873, https://doi.org/10.1373/clinchem.2010.157438.

[31] B. Lu, K. Kurmi, |M. Munoz-Gomez, E.J.J. Ambuludi, et al., Impaired β-cell glucokinase as an underlying mechanism in diet-induced diabetic mice, Dis. Model Mech. 11 (2018), https://doi.org/10.1242/dmm.033316.